Incommensurate Numbers, Continued Fractions, and Fractal Immittances

A. Lakhtakia *, R. Messier *·**, V. V. Varadan *, and V. K. Varadan *

The Pennsylvania State University, University Park, PA 16802 (USA)

Continued fractions have a rich tradition in the theory of numbers; e.g., non-terminating continued fractions represent irrational numbers. It will be shown that a class of continued fractions possess the property of self-referential decomposition, and their interpretation in the form of non-terminating ladder circuits gives rise to fractal immittances with potential analogies to rough surfaces, thin cermet films, as well as to the internal void network structure of thick films.

Introduction

The motivation for this work comes from number theory: the representation of irrational numbers in the Stieltjes continued fraction form, and which has already inspired the development of ladder circuits [1]. Continued fractions have recently been used in understanding fractal quantization of particles in one-dimensional potentials with incommensurate periods [2], as well as in two-dimensional electron gases [3]: a particularly appealing and simple interpretation of the relevant Hamiltonian has been given by Chao [4]. Continued fractions have also been applied in examining the frustrated instabilities of active optical resonators [5].

Although continued fractions have seen some use in the characterisation of the rough surfaces of real materials [6, 7], they have not been applied yet to the inhomogeneous internal structure of materials. It will be shown that specific examples of the resulting ladder circuits have fractal immittances with potential analogies to both cermet thin films and films with internal void networks; and, hence, to the related film properties.

Continued Fractions and Quadratic Irrational Numbers

Any rational or irrational number can be written down in the continued fraction form as [8]

$$\langle a_0, a_1, a_2, a_3, \ldots \rangle = a_0 + \cfrac{1}{a_1 + \cfrac{1}{a_2 + \cfrac{1}{a_3 + \ldots}}}, \qquad (1)$$

with a_0, a_1, etc. being positive integers [but see Appendix]. The continued fraction is finite in size when it represents any rational number p/q, with a_0 being the integral part of the ratio p/q; it turns out that every *rational* number has exactly two such representations [9]. On the other hand, *irrational* numbers have continued fraction representations which are infinite in size. Of these irrational numbers, there is a class of *quadratic irrational* numbers which are solutions of a quadratic equation. A theorem due to Lagrange [10] states that the continued fraction expansion of any quadratic irrational is periodic after a certain state, e.g.,

$$\sqrt{15} = \langle 3, 1, 6, 1, 6, 1, 6, \ldots \rangle,$$

$$\sqrt{31} = \langle 5, 1, 1, 3, 5, 3, 1, 1, 10, 1, 1, 3, 5, 3, 1, 1,$$
$$10, 1, 1, 3, 5, 3, 1, 1, 10, \ldots \rangle,$$

$$\{24 - \sqrt{15}\}/17 = \langle 1, 5, 2, 3, 2, 3, 2, 3, \ldots \rangle.$$

It is the representation of quadratic irrational numbers which is of particular interest in the present context. The simplest example is the number

$$Q(\mu) = \langle 0, \mu, \mu, \mu, \ldots \rangle; \qquad \mu > 0, \qquad (2)$$

---

* Department of Engineering Science and Mechanics.
** Materials Research Laboratory.

Reprint requests to Prof. R. Messier, Engineering Science and Mechanics, 265 Materials Research Labroatory, The Pennsylvania State University, University Park, PA 16802, USA

in which we will accept μ as any rational number; Q can achieve two numerical values *via* the equation $Q = 1/(\mu + Q)$. The next example is the number

$$Q(\mu_1, \mu_2) = \langle 0, \mu_1, \mu_2, \mu_1, \mu_2, \ldots \rangle;$$
$$\mu_1, \mu_2 > 0, \tag{3}$$

which too can achieve two numerical values *via* the quadratic equation $\mu_1 Q^2 + \mu_1 \mu_2 Q - \mu_2 = 0$.

This latter function $Q(\mu_1, \mu_2)$ forms the basis of the work reported here. We will remove the restriction that μ_1 and μ_2 be real positive rational numbers, and let them represent (complex) impedances Z and admittances Y; we will also assume [see Appendix] that all continued fractions are either finite in size or they converge. The first fundamental form comes out when we set $\mu_1 = Y_b = 1/Z_b$ and $\mu_2 = Z_a = 1/Y_a$, so that

$$Q(Y_b, Z_a) = 0 + \cfrac{1}{Y_b + \cfrac{1}{Z_a + \cfrac{1}{Y_b + \ldots}}}, \tag{4}$$

and $Q(Y_b, Z_a) + Z_a$ can be interpreted as the *impedance* of the "series-parallel" circuit shown in Figure 1 a. The second fundamental form comes around when $\mu_1 = Z_b$ and $\mu_2 = Y_a$ so that

$$Q(Z_b, Y_a) = 0 + \cfrac{1}{Z_b + \cfrac{1}{Y_a + \cfrac{1}{Z_b + \ldots}}}, \tag{5}$$

and $Q(Z_b, Y_a) + Y_a$ can be interpreted as the *admittance* of the "parallel-series" circuit shown in Figure 1 b.

From the preceding paragraph, it is immediately obvious that $Q(Y_b, Z_a) + Z_a$ and $Q(Z_b, Y_a) + Y_a$ are nothing but the immittances of ladder circuits [1]. Usually, however, ladder circuits are terminated in some prescribed fashion; thus, their immittances are "closer" to rational numbers than to irrational numbers.

Circuits of Infinite Size: Impedances

There is no restriction on ladder circuits that they be terminated after some number of stages, and we seize upon that idea to generalize $Q(Y_b, Z_a) + Z_a$. Our basic building blocks are two impedances $Z_a = 1/Y_a$ and $Z_b = 1/Y_b$, and the circuit will be constructed in a sequential manner. At the zeroth stage, these imped-
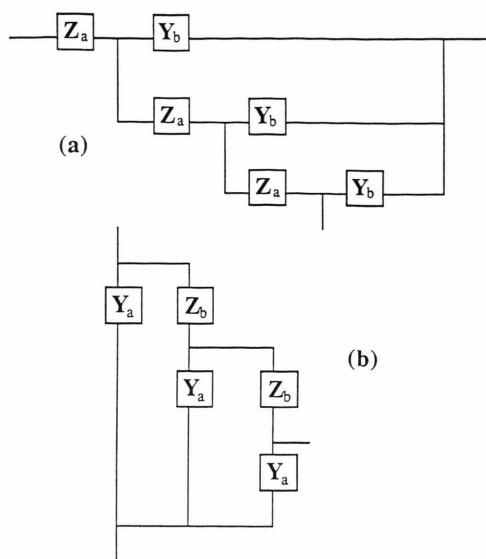

Fig. 1. Ladder circuit representation of (a) $Q(Y_b, Z_a) + Z_a$ in the "series-parallel" form, and (b) $Q(Z_b, Y_a) + Y_a$ in the "parallel-series" form.

ances are connected in series, and

$$Z^{(0)} = Z_a + Z_b. \tag{6a}$$

Then Z_b is shorted by N_1 parallel branches, each of which carries an impedance $p_1 Z_a$ and $q_1 Z_b$, where p_1 and q_1 are appropriate numbers such that $p_1 Z_a$ and $q_1 Z_b$ are realizable. Consequently, the impedance of the circuit at this stage can be represented by

$$Z^{(1)} = Z_a + \cfrac{1}{Y_b + \cfrac{N_1}{p_1 Z_a + q_1 Z_b}}. \tag{6b}$$

In the next stage of growth each of the impedances $q_1 Z_b$ is shorted out by N_2 parallel branches, each having an impedance $p_2 Z_a + q_2 Z_b$. Thus, the circuit impedance at this stage is given as

$$Z^{(2)} = Z_a + \cfrac{1}{Y_b + \cfrac{N_1}{p_1 Z_a + \cfrac{1}{Y_b/q_1 + \cfrac{N_2}{p_2 Z_a + q_2 Z_b}}}}. \tag{6c}$$

This process continues *ad infinitum*. Provided the real and the imaginary parts of the sequence $\{Z^{(i)}\}$ converge, it can be said that

$$Z^{(\infty)} = \lim_{i \to \infty} Z^{(i)} \tag{6d}$$

will be the impedance of the circuit so obtained. There is a pattern immediately obvious in the development of this circuit. As an example, let $N_i = N$ and $p_i = q_i = a^i \; \forall i \geq 1$. Then, it is easy to verify that

$$Z^{(i)} = Z_a + 1/[Y_b + (N/a) \, Y^{(i-1)}]; \quad i > 0, \quad (7\,a)$$

in which $Y^{(i)} = 1/Z^{(i)} \; \forall i \geq 0$. Provided (6d) holds, then it can be easily seen that $Z^{(\infty)}$ can be obtained as a solution of the quadratic equation

$$[Z^{(\infty)}]^2 \, Y_b + [Z^{(\infty)}] \, \{N/a - Z_a \, Y_b - 1\}$$
$$- Z_a \, N/a = 0. \quad (7\,b)$$

This scheme for generating $Z^{(\infty)}$ can be easily randomised by randomizing the selection of N_i, p_i and q_i. It may be that some of the circuits will turn out to be fractal, and others may not be so; and we are *a priori* unable to decisively rule on the outcome. Instead, we will give four examples which will be shown to have *fractal* impedances in the frequency domain, provided some specific conditions have been satisfied. These cases are:

Circuit ZRC: $\forall i \geq 1, N_i = N, p_i = a^i, q_i = 1; \; a > 1$; $Z_a = R$ and $Z_b = [j \omega C]^{-1}$.

For this circuit, by substitution of these conditions in (6) and computing $Z^{(\infty)}$ it can be shown that the following *scaling* relationships in the frequency domain arise:

$$Z^{(\infty)}(\omega) = R + a Z^{(\infty)}(a \omega) \quad (8\,a)$$
$$\cdot [N + a [j \omega C] Z^{(\infty)}(a \omega)]^{-1},$$

$$Z^{(\infty)}(\omega/a) = R + a Z^{(\infty)}(\omega)$$
$$\cdot [N + [j \omega C] Z^{(\infty)}(\omega)]^{-1}. \quad (8\,b)$$

Circuit ZCR: $\forall i \geq 1, N_i = N, p_i = a^i, q_i = 1; \; a > 1$; $Z_a = [j \omega C]^{-1}$ and $Z_b = R$.

$$Z^{(\infty)}(\omega) = [j \omega C]^{-1} + a Z^{(\infty)}(\omega/a)$$
$$\cdot [N + R^{-1} Z^{(\infty)}(\omega/a)]^{-1}, \quad (9\,a)$$

$$a Z^{(\infty)}(a \omega) = [j \omega C]^{-1} + a Z^{(\infty)}(\omega)$$
$$\cdot [N + R^{-1} Z^{(\infty)}(\omega)]^{-1}. \quad (9\,b)$$

Circuit ZRL: $\forall i \geq 1, N_i = N, p_i = a^i, q_i = 1; \; a > 1$; $Z_a = R$ and $Z_b = j \omega L$.

$$Z^{(\infty)}(\omega) = R + a Z^{(\infty)}(\omega/a) \quad (10\,a)$$
$$\cdot [N + a [j \omega L]^{-1} Z^{(\infty)}(\omega/a)]^{-1},$$

$$Z^{(\infty)}(a \omega) = R + a Z^{(\infty)}(\omega)$$
$$\cdot [N + [j \omega L]^{-1} Z^{(\infty)}(\omega)]^{-1} \quad (10\,b)$$

Circuit ZLR: $\forall i \geq 1, N_i = N, p_i = a^i, q_i = 1; \; a > 1$; $Z_a = j \omega L$ and $Z_b = R$.

$$Z^{(\infty)}(\omega) = j \omega L + Z^{(\infty)}(a \omega)$$
$$\cdot [N + R^{-1} Z^{(\infty)}(a \omega)]^{-1}, \quad (11\,a)$$

$$a Z^{(\infty)}(\omega/a) = j \omega L + a Z^{(\infty)}(\omega)$$
$$\cdot [N + R^{-1} Z^{(\infty)}(\omega)]^{-1}, \quad (11\,b)$$

It should be noted that in all of these four cases, the parameter a assumes a special status: as the discriminant for scale over the frequency range ω. To further elucidate the self-referential character of such circuits, consider the case when $N = 1$ and when Z_a as well as Z_b are arbitrary impedances. Then, it is possible to see that while $Z^{(0)} = Z_a + Z_b$, the higher order approximants can be set down compactly as

$$Z^{(i)} = [Z^{(0)} z_{1,i} + a Z_a Z^{(0)} + Z_a Z_b]$$
$$\cdot [a Z_a + Z_b + z_{1,i}]^{-1}, \quad i \geq 1, \quad (12)$$

in which

$$z_{1,1} = Z_b, \quad (13\,a)$$

but

$$z_{1,i} = Z_b [a^2 Z_a + z_{2,i}] \cdot [a^2 Z_a + Z_b + z_{2,i}]^{-1},$$
$$i \geq 2. \quad (13\,b)$$

But the impedance functions $z_{2,i}, i \geq 2$, can themselves be further simplified with the help of the impedance functions $z_{3,i}, i \geq 3$, as

$$z_{2,2} = Z_b, \quad (14\,a)$$

but

$$z_{2,i} = Z_b [a^3 Z_a + z_{3,i}] \cdot [a^3 Z_a + Z_b + z_{3,i}]^{-1},$$
$$i \geq 3. \quad (14\,b)$$

It then becomes possible to observe the self-affinity of these circuits by defining the functions

$$z_{i,i} = Z_b, \quad (15\,a)$$
$$z_{j,i} = 0; \quad \text{if} \quad i < j, \quad (15\,b)$$
$$z_{j,i} = Z_b [a^{j+1} Z_a + z_{j+1,i}] \quad (15\,c)$$
$$\cdot [a^{j+1} Z_a + Z_b + z_{j+1,i}]^{-1}; \quad i \geq j+1.$$

Circuits of Infinite Size: Admittances

The aforementioned circuits are of the "series-parallel" form such as $Q(Y_b, Z_a) + Z_a$ in (4). Because of duality, it is easy to visualise "parallel-series" forms such as $Q(Z_b, Y_a) + Y_a$ in (5). Our building blocks here

will be two admittances $Y_a = 1/Z_a$ and $Y_b = 1/Z_b$. In the zeroth-stage these admittances are connected in parallel; then,

$$Y^{(0)} = Y_a + Y_b. \tag{16a}$$

Next, N_1 branches connected in series are inserted into the branch containing Y_b, each branch of admittance $p_1 Y_a + q_1 Y_b$. Consequently, the admittance of the circuit at this stage can be represented by

$$Y^{(1)} = Y_a + \cfrac{1}{Z_b + \cfrac{N_1}{p_1 Y_a + q_1 Y_b}}, \tag{16b}$$

where $Z_b = 1/Y_b$. In the second stage, N_2 branches connected in series are inserted into the branches containing $q_1 Y_b$, each branch of admittance $p_2 Y_a + q_2 Y_b$; hence,

$$Y^{(2)} = Y_a + \cfrac{1}{Z_b + \cfrac{N_1}{p_1 Y_a + \cfrac{1}{Z_b/q_1 + \cfrac{N_2}{p_2 Y_a + q_2 Y_b}}}}, \tag{16c}$$

This process also continues *ad infinitum*. Provided the real and the imaginary parts of the sequence $\{Y^{(i)}\}$ converge, it can be said that

$$Y^{(\infty)} = \operatorname*{Lim}_{i \to \infty} Y^{(i)} \tag{16d}$$

will be the admittance of the circuit so obtained. As a counterpart to (7a), if $N_i = N$ and $p_i = q_i = a^i \; \forall i \geq 1$, then

$$Y^{(i)} = Y_a + 1/[Z_b + (N/a) Z^{(i-1)}]; \quad i > 0, \tag{17}$$

where $Z^{(i)} = 1/Y^{(i)} \; \forall i \geq 0$.

The "parallel-series" counterparts of the circuits identified above as ZRC, etc., along their respective frequency scaling relationships, are as follows:

Circuit YRC: $\forall i \geq 1, N_i = N, p_i = a^i, q_i = 1; \quad a > 1$;
$Y_a = R^{-1}$ and $Y_b = j \omega C$.

$$Y^{(\infty)}(\omega) = R^{-1} + a Y^{(\infty)}(\omega/a) \tag{18a}$$
$$\cdot [N + a[j \omega C]^{-1} Y^{(\infty)}(\omega/a)]^{-1},$$

$$Y^{(\infty)}(a\omega) = R^{-1} + a Y^{(\infty)}(\omega) \tag{18b}$$
$$\cdot [N + [j \omega C]^{-1} Y^{(\infty)}(\omega)]^{-1}.$$

Circuit YCR: $\forall i \geq 1, N_i = N, p_i = a^i, q_i = 1; \quad a > 1$;
$Y_a = j \omega C$ and $Y_b = R^{-1}$.

$$Y^{(\infty)}(\omega) = j \omega C + Y^{(\infty)}(a\omega)$$
$$\cdot [N + R \, Y^{(\infty)}(a\omega)]^{-1}, \tag{19a}$$

$$a \, Y^{(\infty)}(\omega/a) = j \omega C + a \, Y^{(\infty)}(\omega)$$
$$\cdot [N + R \, Y^{(\infty)}(\omega)]^{-1}, \tag{19b}$$

Circuit YRL: $\forall i \geq 1, N_i = N, p_i = a^i, q_i = 1; \quad a > 1$;
$Y_a = R^{-1}$ and $Y_b = [j \omega L]^{-1}$.

$$Y^{(\infty)}(\omega) = R^{-1} + a \, Y^{(\infty)}(a\omega) \tag{20a}$$
$$\cdot [N + a[j \omega L] \, Y^{(\infty)}(a\omega)]^{-1},$$

$$Y^{(\infty)}(\omega/a) = R^{-1} + a \, Y^{(\infty)}(\omega)$$
$$\cdot [N + [j \omega L] \, Y^{(\infty)}(\omega)]^{-1}, \tag{20b}$$

Circuit YLR: $\forall i \geq 1, N_i = N, p_i = a^i, q_i = 1; \quad a > 1$;
$Y_a = [j \omega L]^{-1}$ and $Y_b = R^{-1}$.

$$Y^{(\infty)}(\omega) = [j \omega L]^{-1} + Y^{(\infty)}(\omega/a)$$
$$\cdot [N + R \, Y^{(\infty)}(\omega/a)]^{-1}, \tag{21a}$$

$$a \, Y^{(\infty)}(a\omega) = [j \omega L]^{-1} + Y^{(\infty)}(\omega)$$
$$\cdot [N + R \, Y^{(\infty)}(\omega)]^{-1}. \tag{21b}$$

By making use of the interchanges $Z \Leftrightarrow Y$, $R \Leftrightarrow R^{-1}$ and $L \Leftrightarrow C$, it is easy to show that the circuits YRC, YCR, YRL and YLR are the duals, respectively, of the circuits ZRL, ZLR, ZRC and ZCR.

Discussion

For the remainder of this paper, we will confine our discussion to the circuits ZRC and ZCR, whose scaling behavior are, respectively, identified by (8a, b) and (9a, b); furthermore, we shall drop the superscript (∞) on Z.

First, the circuit ZRC and a couple of its possible applications. Shown in Fig. 2 are the plots of the real and the imaginary parts of $Z^{(i)}$ as well as the phase angle $\varphi^{(i)} = \arctan [\operatorname{Im}\{Z^{(i)}\}/\operatorname{Re}\{Z^{(i)}\}]$ as functions of the frequency ω; the building blocks are $R = 1 \text{ k}\Omega$ and $C = 1 \text{ nF}$. To be noted is the fact that Z can be extrapolated from these graphs. It can be seen that in the low-frequency regime ($\omega RC \ll 1$), both the real and the imaginary parts of Z are proportional to $\omega^{-\zeta}$, where $\zeta = 1 - \ln(N)/\ln(a) = 1 - D$, D being the fractal dimension [12]; indeed $Z(\omega)$ is actually proportional to $(i\omega)^{-\zeta}$. As the frequency increases, then this law is no longer followed: for the high-frequency regime ($\omega RC \gg 1$), the real part of Z approaches the constant
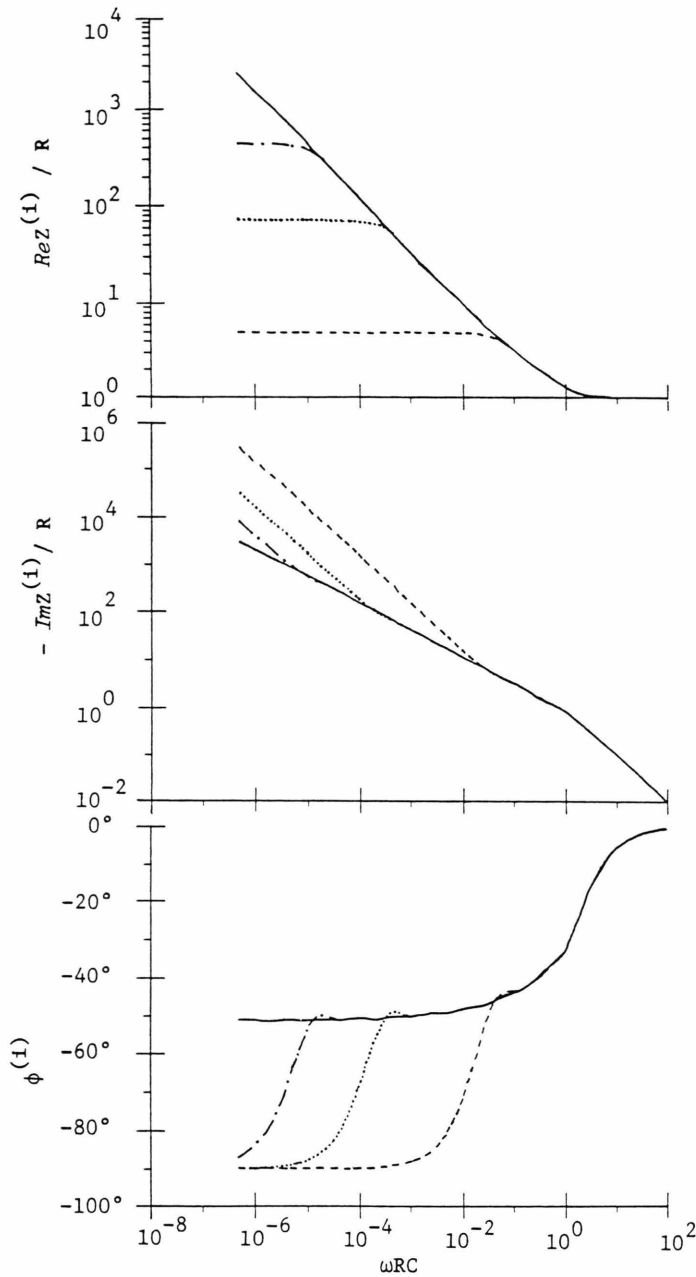
Fig. 2. Plots of Re $\{Z^{(i)}/R\}$, $-$ Im $\{Z^{(i)}/R\}$ and phase angle $\varphi^{(i)} =$ arctan [Im $\{Z^{(i)}\}$/Re $\{Z^{(i)}\}$] against frequency ω for the circuit ZRC. The building blocks $R = 1\,\mathrm{k\Omega}$ and $C = 1\,\mathrm{nF}$; the branch number $N = 2$ and the branching parameter $a = 5$, $i = 2$ (– – –), 5 ($\cdots$), 7 (–·–·–) and 10 (——). Note that $a > N^2$ and that for $\omega RC \ll 1$, $Z(\omega) \sim (i\omega)^{-\zeta}$, where $\zeta = 1 - \ln(N)/\ln(a)$.
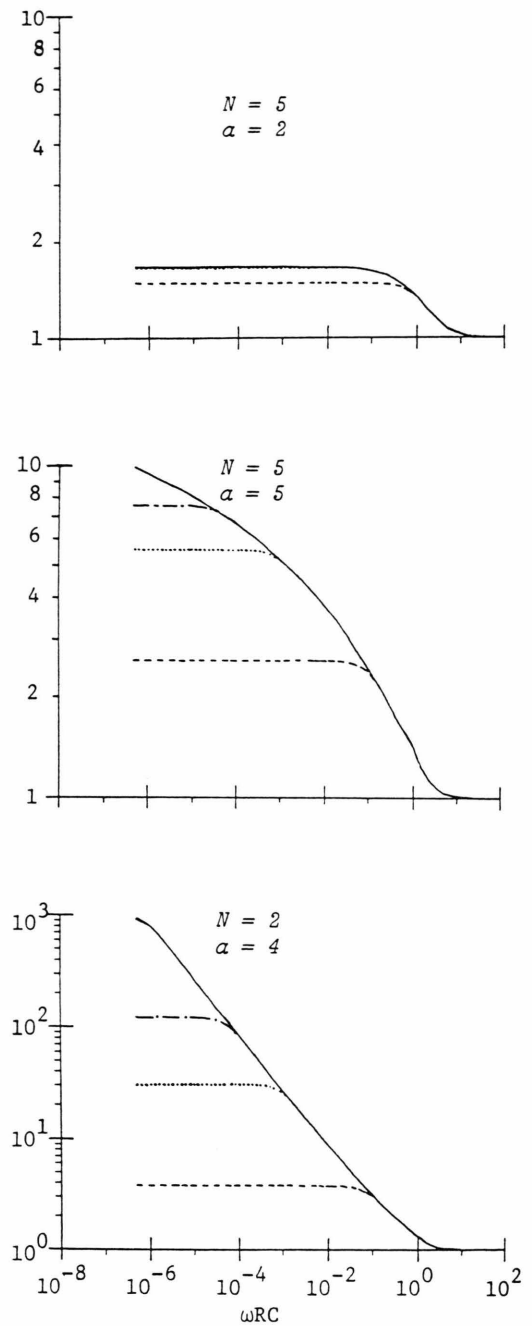
Fig. 3. Plots of Re $\{Z^{(i)}/R\}$ against frequency ω for the circuit ZRC. The building blocks $R = 1\,\mathrm{k\Omega}$ and $C = 1\,\mathrm{nF}$; $i = 2$ (– – –), 5 ($\cdots$), 7 (–·–·–) and 10 (——). Three cases have been considered: (a) $a = 2$, $N = 5$, (b) $a = N = 5$, and (c) $a = 4$, $N = 2$.

resistance R and the imaginary part of Z decays as ω^{-1}. But the imaginary part of Z is very small when compared to its real part; hence, Z is almost purely resistive at high frequencies. This behavior of the ZRC circuit was first noted by Liu [6] for $N = 2$, and the low-frequency, constant-phase-angle response of the ZRC circuit makes it a plausible model for some electrode surfaces [11, 13].

It should be noted that in the calculations of Fig. 2, $a > N$. Furthermore, $\ln(N)/\ln(a)$ is a fractal dimension of the ZRC circuit and lies between 0 and 0.5. Since the circuit has been used to encode in it the topography of an electrode surface, this consideration is justified [7]. From the point of view of circuit topology, however, there is no reason to confine $N < a$. In Figs. 3 and 4, the calculations of Fig. 2 are repeated for varying values of the ratio a/N. From these and other studies, it appears that the low-frequency, constant-phase-angle response of the circuit ZRC is confined to the regime $a \geq N^2$. When $N \gg a$, however, another interesting characteristic appears: whereas for $\omega RC \gg 1$, $Z \cong R$, even in the low-frequency regime Z is almost purely resistive. As the parameter a is increased relative to N^2, this behavior is supplanted by the "fractal" behavior observed for $a \geq N^2$.

As an application of the circuit ZRC, we now consider the reflection coefficient $\Re(\omega)$ when a planewave is normally incident on an infinite plane [14] whose impedance can be modelled by that of the ZRC circuit;

$$\Re(\omega) = [Z(\omega) - \eta_0][Z(\omega) + \eta_0]^{-1}. \qquad (22)$$

This reflection coefficient is plotted in Figs. 5 and 6 with $R = 200\,\Omega$ and $C = 100\,\text{pF}$; the free space impedance, $\eta_0 = 120\,\pi\,\Omega > R$. In Fig. 5 the condition $a \geq N^2$ has been fulfilled. For this case, it appears that in the low-frequency range, the reflection coefficient is almost equal to $+1$, but in the high-frequency regime it acquires a constant negative value. Neither of these results is surprising because for $\omega RC \ll 1$, $|Z(\omega)| \gg \eta_0$, the free-space impedance; while for $\omega RC \gg 1$, $Z(\omega) \cong R < \eta_0$. In other words, at low frequencies the impedance plane behaves as if it were a perfect magnetic conductor (PMC), but becomes an insulator at higher frequencies. It is to be concluded, therefore, that the ZRC circuit with $a \geq N^2$ is a plausible model for PMC-insulator transition. When $a \ll N^2$, the circuit ZRC also provides a model for such transitions, but somewhat of a different kind. Shown in Fig. 6 is the case when $a = 2$ and $N = 5$. From this figure, it is to
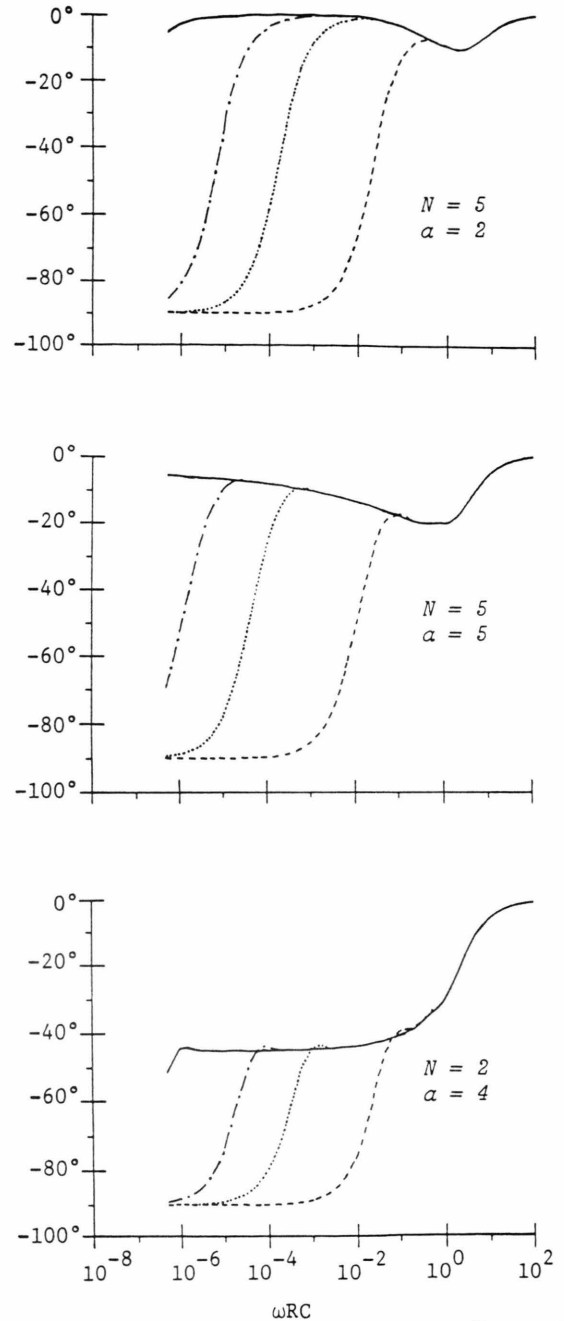

Fig. 4. Plots of phase angle $\varphi^{(i)} = \arctan[\text{Im}\{Z^{(i)}\}/\text{Re}\{Z^{(i)}\}]$ against frequency ω for the circuit ZRC. See Fig. 3 for other details.

be noted that both in the low- and the high-frequency regimes, $\Re(\omega)$ is almost always a negative real number (except for the static case when it equals unity), which is because $Z(\omega)$ is almost purely resistive in these frequency ranges. Thus, this appears to be a case of
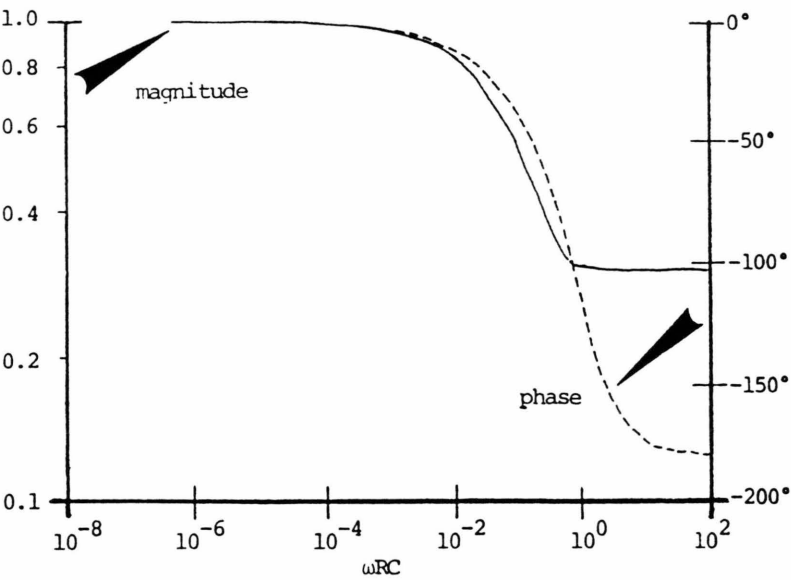
Fig. 5. Magnitude and phase of the reflection coefficient $\Re(\omega)$ given as a function of ω by (22). The impedance $Z(\omega)$ of the ZRC circuit is approximated by $Z^{(10)}$, no difference being observed when $Z^{(7)}$ was used in place of $Z(\omega)$. The parameters $R = 200\,\Omega$, $C = 100$ pF, $a = 5$, and $N = 2$.

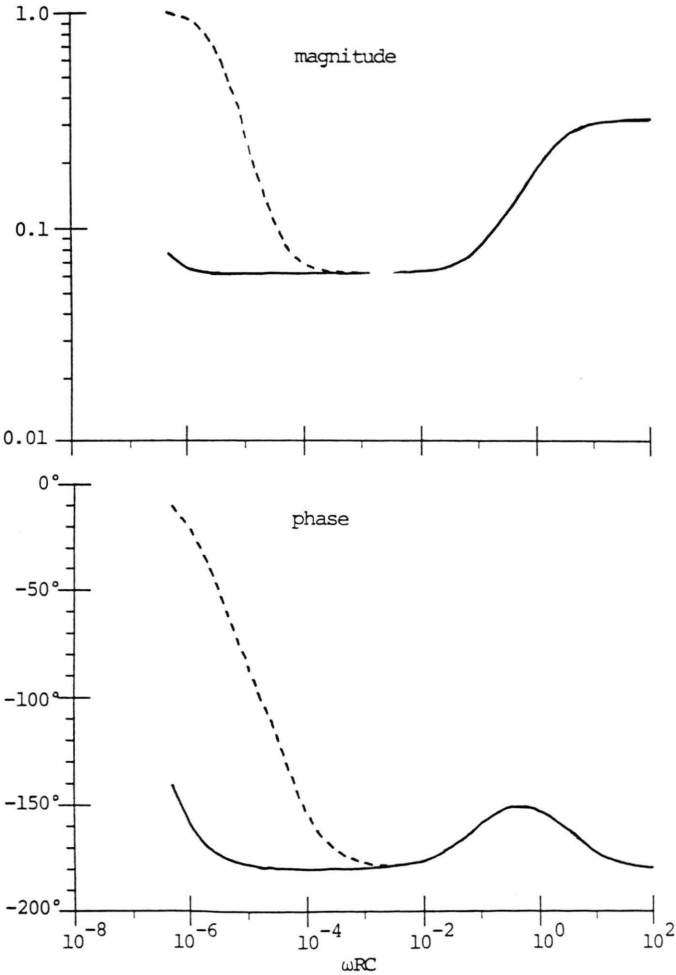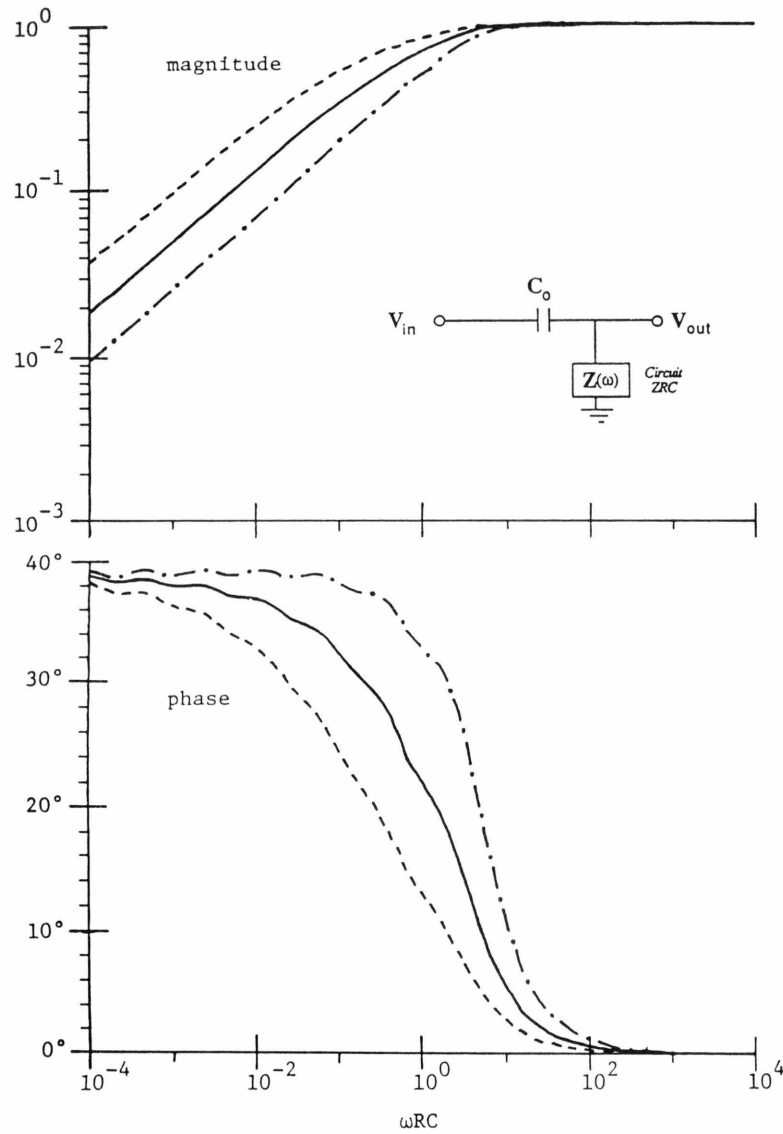Fig. 6. Magnitude and phase of $\Re(\omega)$ given as a function of ω by (22). The impedance $Z(\omega)$ of the circuit ZRC was approximated by $Z^{(7)}(---)$ and $Z^{(10)}(\text{——})$. The parameters $R = 200\Omega$, $C = 100$ pF, $a = 2$, and $N = 5$.

Fig. 7. Magnitude and phase of $G(\omega)$ given as a function of ω by (23). The impedance $Z(\omega)$ of the circuit ZRC was approximated by $Z^{(10)}$ with $R = 1\,k\Omega$, $C = 100\,pF$, $a = 5$ and $N = 2$. The capacitance $C_0 = C/2$ (−·−·−), C (——) and $2C$ (   ).
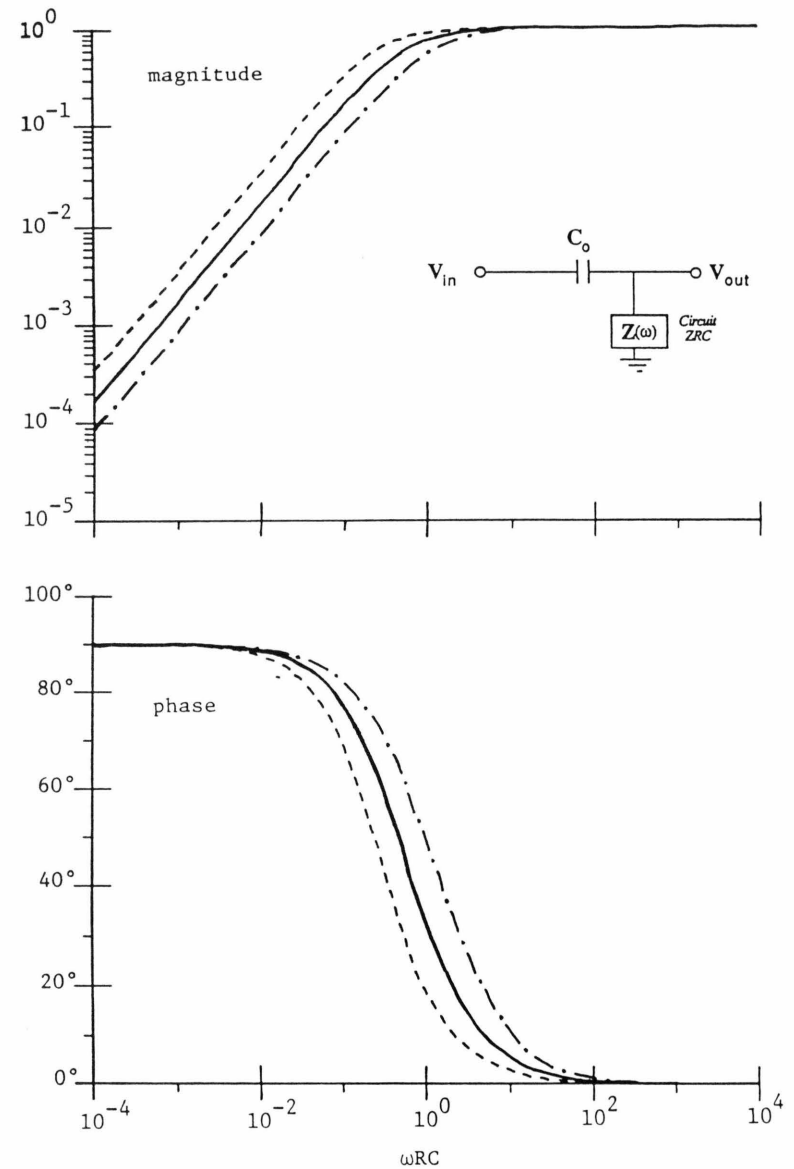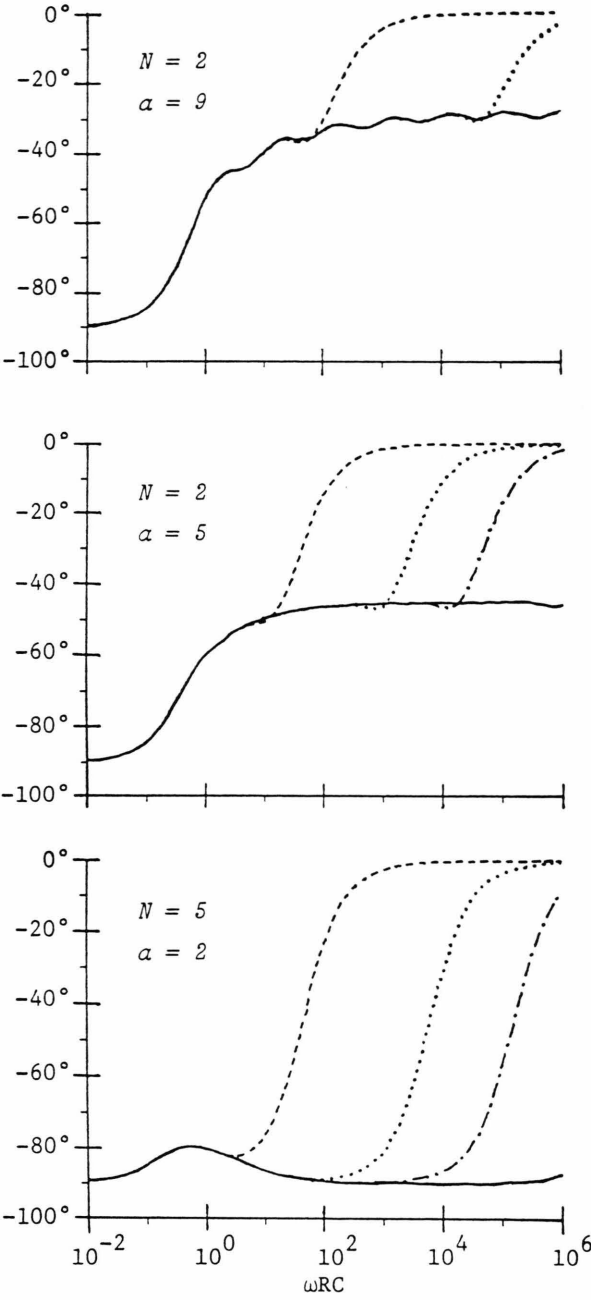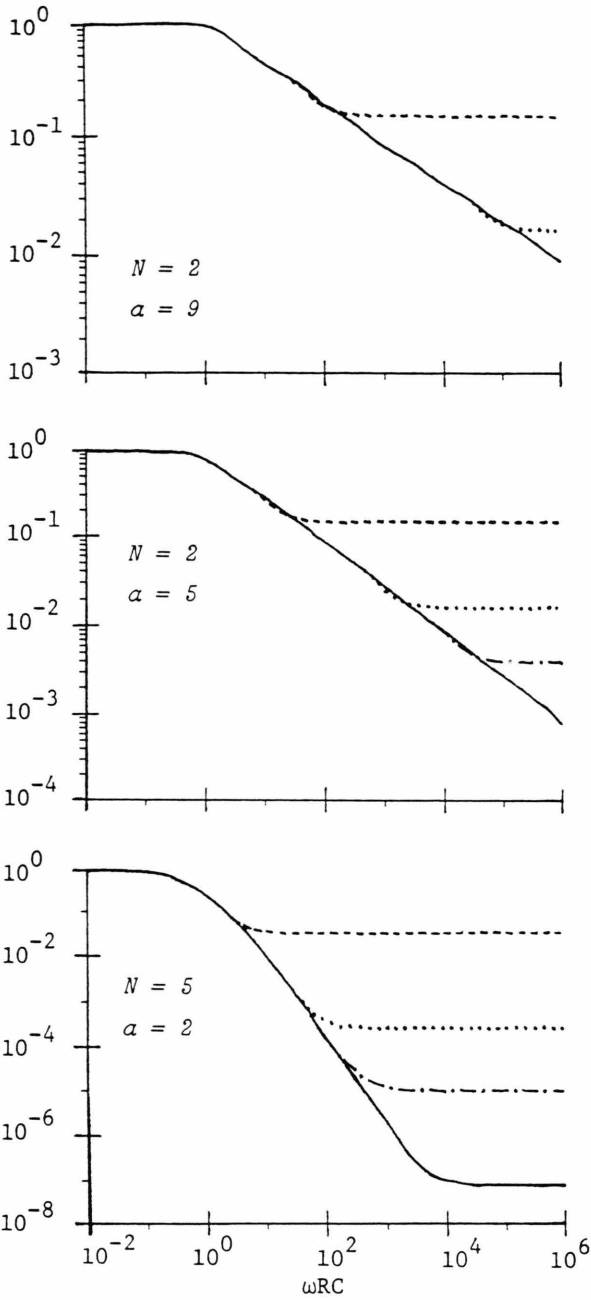
Fig. 8. Same as Fig. 7, except $a = 2$ and $N = 5$.

Fig. 9. Plots of $\text{Re}\{Z^{(i)}/R\}$ against frequency ω for the circuit ZCR. The building blocks $R = 1\,\text{k}\Omega$ and $C = 1\,\text{nF}$; $i = 2\,(---)$, $5\,(\cdots)$, $7\,(-\cdot-\cdot-)$ and $10\,(\text{———})$. Three cases have been considered: (a) $a = 9$, $N = 2$, (b) $a = 5$, $N = 2$, and (c) $a = 2$, $N = 5$.

Fig. 10. Plots of phase angle $\varphi^{(i)} = \arctan[\text{Im}\{Z^{(i)}\}/\text{Re}\{Z^{(i)}\}]$ against frequency ω for the circuit ZCR. See Fig. 9 for other details.

insulator-insulator transition, perhaps typifying a curious (relaxation?) mechanism in which the dielectric constant changes from a low value to a higher value as the frequency increases [15, 16]. Parenthetically, it should be noted that this second case can also be interpreted to be symptomatic of a relaxation in which the (magnetic) permeability changes from a high value to a lower one with the increase in frequency [17]. Both of these impedance plane models merit further attention. It must also be noted that the scattering plane need not be planar: it is possible to think of a rough, bimaterial interface as a perfectly smooth plane possessed with a space-dependent impedance [18]. This impedance is not only a function of the geometry of the actual (rough) surface, but also of the frequency ω and the field incident on the surface.

Finally, the circuit ZRC may be used as part of a filter, as shown in the insets of Figs. 7 and 8. For these two figures, the open-circuit voltage gain was computed via

$$G(\omega) = Z(\omega) [Z(\omega) + (j \omega C_0)^{-1}], \qquad (23)$$

in which $Z(\omega)$ was approximated by $Z^{(10)}(\omega)$, $R = 1\,\mathrm{k}\Omega$ and $C = 100\,\mathrm{pF}$. The capacitance C_0 was assumed to have three values: $C_0 = C/2$, C and $2C$. In Fig. 7, $a = 5$ and $N = 2$, so that $a > N^2$; and in the latter figure, $a = 2$ and $N = 5$ so that $a \ll N^2$. It is to be noted that for either case, $G(\omega) \cong 1$ when $\omega RC \gg 1$, so that the high frequencies are passed on by the filters without any distortion. The low frequencies ($\omega RC \ll 1$) are, however, attenuated, so that these filters are essentially high pass; furthermore, the roll-off appears to be rather insensitive to the capacitance ratio C_0/C. But the roll-off in Fig. 7 is about 8.4 dB/decade, and in Fig. 8 it is about 20 dB/decade, which suggests that as an element of these filters, the circuit ZRC with $a \ll N^2$ is certainly the more efficient one. This is because, as evinced by Fig. 3, the circuit ZRC with $a \ll N^2$ behaves much like a pure resistance in both the low- and the high-frequency ranges.

Just as the response of the circuit ZRC is dominated by its real (resistive) part, the circuit ZCR is dominated by its imaginary (capacitative) part. Shown in Figs. 9 and 10 are the plots of the real part and the
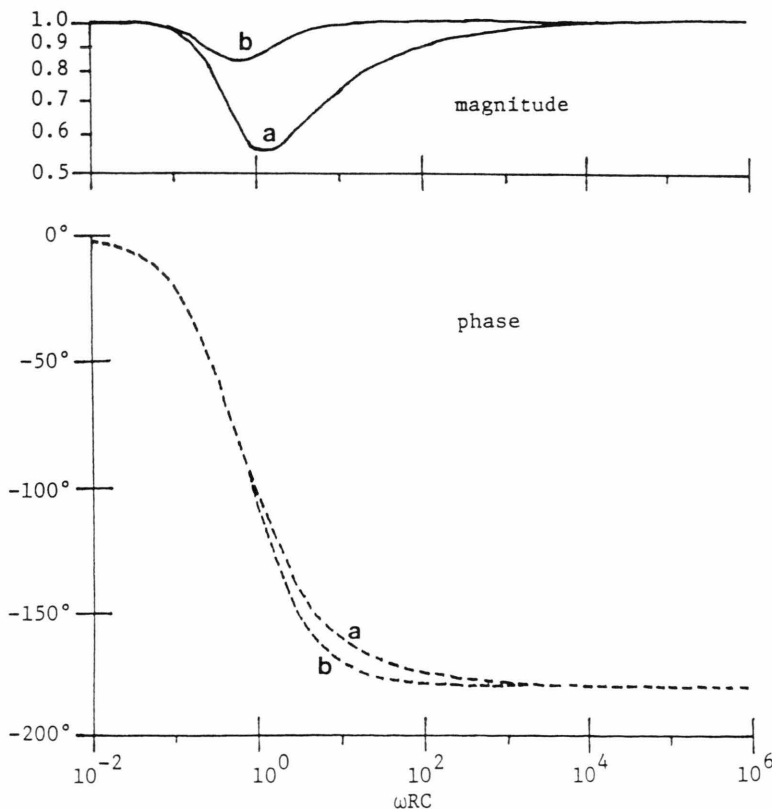

Fig. 11. Magnitude and phase of the reflection coefficient $\mathfrak{R}(\omega)$ given as a function of ω by (22). The impedance $Z(\omega)$ of the ZCR circuit is approximated by $Z^{(10)}$, no difference being observed when $Z^{(7)}$ was used in place of $Z(\omega)$; $R = 200\,\Omega$, $C = 100\,\mathrm{pF}$. The branching parameters are (a) $a = 5$, $N = 2$, and (b) $a = 2$, $N = 5$.
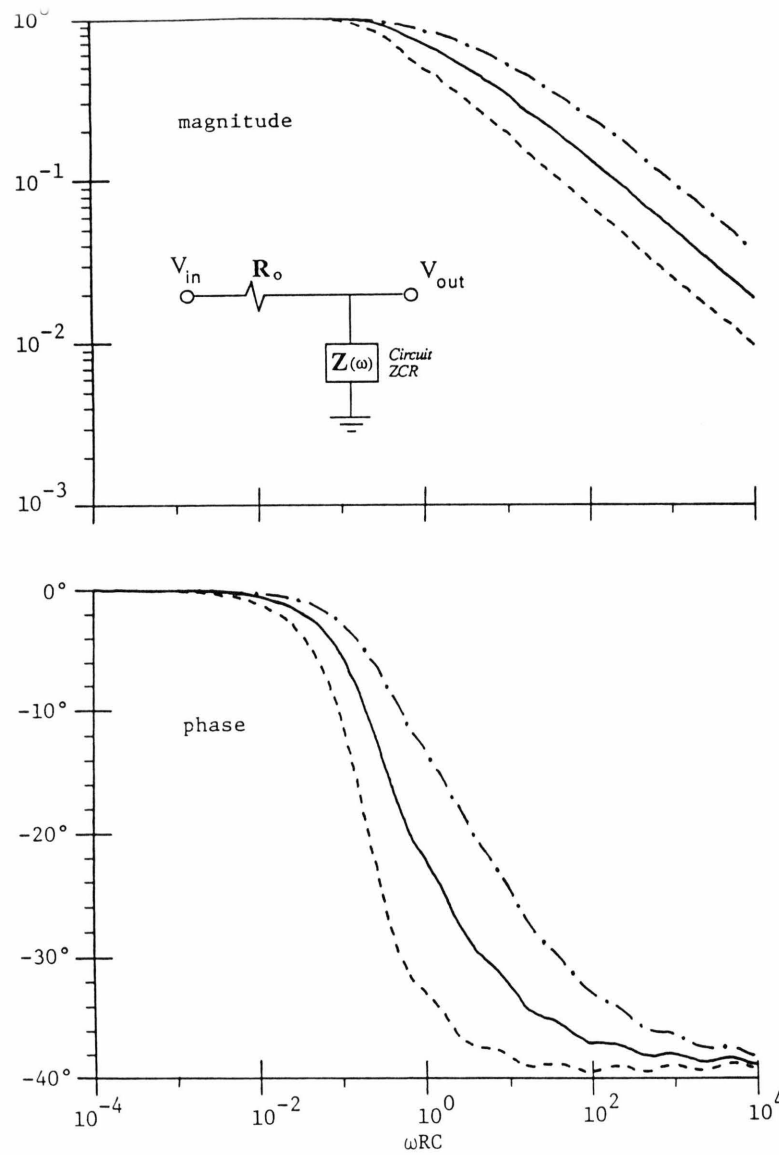
Fig. 12. Magnitude and phase of $G(\omega)$ given as a function of ω by (23). The impedance $Z(\omega)$ of the circuit ZCR was approximated by $Z^{(10)}$ with $R = 1$ kΩ, $C = 100$ pF, $a = 5$ and $N = 2$. The resistance $R_0 = R/2$ ($-\cdot-\cdot-$), R ($\longrightarrow$) and $2R$ ($---$).
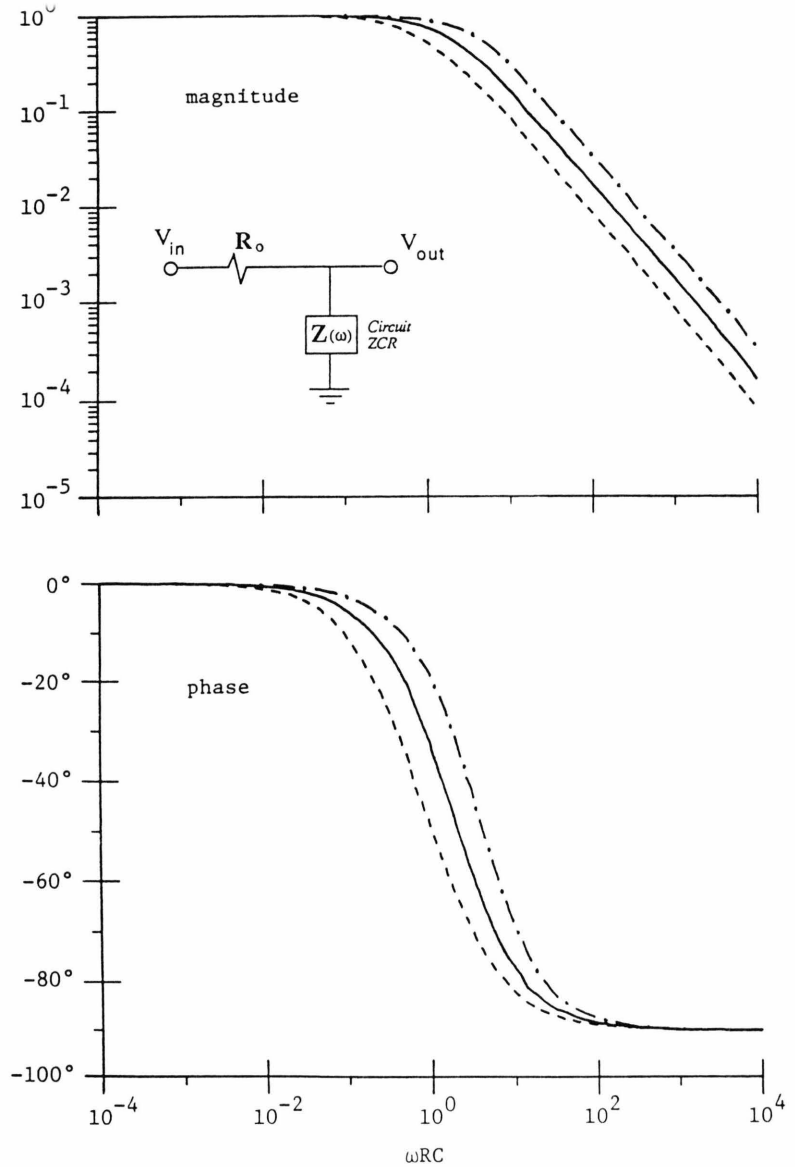
Fig. 13. Same as Fig. 12, except $a = 2$ and $N = 5$.

phase, respectively, of the approximants $Z^{(i)}$ for some circuits ZCR; the building blocks are $R = 1 \, k\Omega$ and $C = 1 \, nF$. To be noted is the fact that in the static limit $\omega \to \infty$, $Z(\omega)$ is almost purely capacitive. Furthermore, $\mathrm{Re}\, Z(\omega) = R$ at low frequencies ($\omega RC \ll 1$), but for $\omega RC \gg 1$, it appears that $\mathrm{Re}\, Z(\omega)$ is proportional to $\omega^{-\zeta}$. When $a \geq N^2$, then $\zeta = \ln(N)/\ln(a)$, which is a number less than 0.5; as the ratio N/a increases, however, ζ does so too and achieves values higher than unity. For $a \geq N^2$, the impedance of the circuit ZCR also scales as $(i\omega)^{-\zeta}$ for $\omega RC \gg 1$, but this relationship becomes slightly imprecise in its phase when $a \gg N^2$. On the other hand, when $a \ll N^2$, then both in the low and the high frequency limits, $Z(\omega)$ is almost purely capacitive.

Using (22), the reflection coefficient $\mathfrak{R}(\omega)$ is computed in Fig. 11 for a planewave normally incident on an infinite plane whose impedance is modelled by the circuit ZCR; $R = 200\,\Omega$ and $C = 100\,pF$. It is apparent from this figure that, qualitatively speaking, there is no difference between the cases (a) $a \geq N^2$ and (b) $a \ll N^2$. In the low frequency range, $\mathfrak{R}(\omega)$ tends towards $+1$; and in the high frequency regime, $\mathfrak{R}(\omega)$ is approximately equal to negative unity. Both of these observations are consistent with the capacitive nature of the circuit ZCR. Also, it appears that the impedance plane behaves as a perfect electric conductor (PEC) for $\omega RC \gg 1$, so that the circuit ZCR models PMC-PEC transitions, regardless of the specific values of the branching parameters a and N. Pertinent to the scattering of acoustic waves, this can also be interpreted as a transition from an acoustically hard surface to an acoustically soft one.

The open-circuit voltage gain $G(\omega)$ of the filter, shown in the insets of Figs. 12 and 13, has been computed via the relationship (23). For these calculations, $Z(\omega)$ of the circuit ZCR was approximated by $Z^{(10)}(\omega)$, $R = 1\,k\Omega$ and $C = 100\,pF$. The resistance R_0 was assumed to have three values: $R_0 = R/2$, R and $2R$. In Fig. 12, $a = 5$ and $N = 2$, so that $a > N^2$; while in Fig. 13, $a \ll N^2$ and $a = 2$ with $N = 5$. It is to be noted that for either case, $G(\omega) \cong 1$ when $\omega RC \ll 1$: this implies that the low frequencies are passed on by the filters without any significant distortion. On the other hand, the high frequencies ($\omega RC \gg 1$) are attenuated, the attenuation being rather insensitive to the ratio R_0/R. But this roll-off rate in Fig. 12 is about 8.5 dB/decade, while in Fig. 13 it is almost 20 dB/decade. This suggests that the use of the circuit ZCR with $a \ll N^2$ is certainly more efficient for these low-pass filters.

There are several envisioned applications of this mathematical formalism to the modelling of real thin film materials. First, it has already been shown that the ZRC circuit is a plausible model for the interfacial impedances of rough electrode surfaces in electrochemical cells [6].

Second, cermet films are mixtures of metallic and insulating materials which form a fractal [19–21] sponge-like connected network of either the metallic or the insulator phase, depending upon the concentration of the metal. A test for whether such materials are analogous would be to measure the reflection coefficient of thin (~ 100–$500 \, \text{\AA}$) cermet films when a planewave is normally incident and compare the results with applicable formulas [14] similar to (22). The use of the ZRC and the ZCR circuit impedances to simulate the impedance of an infinite plane should turn out to be analogous to the metallic and the insulating cermet states [20], respectively.

Lastly, for thicker films (1–$100 \, \mu$) of essentially a single-phase material prepared under conditions of low adatom mobility, it has been demonstrated that the top surface is cauliflower-like and is directly related to a conical void network structure [22]. Although these void networks appear fractal, there has been no quantitative description of them [23]. The present work suggests ways to test and measure the fractal nature of such films. The impedances of the void regions and that of the "bulk" conical regions are certainly different; the film properties should have analogy to both the ZRC (ionic diffusion and electrical conductivity) as well as the ZCR (permittivity) circuits.

Acknowledgement

Appendix: Generalized Continued Fractions

Rigorously speaking, a continued fraction should be defined [24] through an ordered set of numbers $\{a_n\}$, $\{b_n\}$ and $\{\zeta_n\}$, where $a_0, a_1, a_2, \ldots$ and $b_1, b_2, \ldots$ are complex numbers with all $b_n \neq 0$, and where $\{\zeta_n\}$ is a sequence in the extended complex plane. The numbers ζ_n approximate the continued fraction z, and assuming that the continued fraction is infinitely long,

$$z = \operatorname*{Lim}_{n \to \infty} \zeta_n, \tag{A1}$$

where

$$\zeta_n = a_0 + \cfrac{b_1}{a_1 + \cfrac{b_2}{a_2 + \dots \atop \dots + b_n/a_n}} \, . \tag{A2}$$

The convergence (A1) is subject to some conditions, which have been discussed in detail in Chaps. 3 and 4 of the book by Jones and Thron [24]. It will suffice for the present purposes to indicate here that the sequence $\{\zeta_n\}$ does converge to z, provided

$$|a_n| \ge |b_n| + 1; \quad n = 1, 2, 3, \dots . \tag{A3}$$

For the sake of computational tractability, it is convenient to express the nth approximant as

$$\zeta_n = B_n/A_n, \tag{A4}$$

where

$$B_{-1} = A_0 = 1, \quad B_0 = a_0, \quad A_{-1} = 0, \tag{A5a}$$

$$A_n = a_n A_{n-1} + b_n A_{n-2}, \quad n = 1, 2, 3\dots, \tag{A5b}$$

$$B_n = a_n B_{n-1} + b_n B_{n-2}, \quad n = 1, 2, 3\dots . \tag{A5c}$$

[1] P. M. Chirlian, Basic Network Theory, McGraw-Hill, New York, 1969, p. 494.
[2] M. Ya. Azbel, Phys. Rev. Lett. **43**, 1954 (1979).
[3] F. D. M. Haldane, Phys. Rev. Lett. **51**, 605 (1983).
[4] K. A. Chao, J. Phys. A **19**, 2907 (1986).
[5] K. Ikeda, M. Mizuno, Phys. Rev. Lett. **53**, 1340 (1984).
[6] S. H. Liu, Phys. Rev. Lett. **55**, 529 (1985).
[7] T. Kaplan, S. H. Liu, and L. J. Gray, Phys. Rev. B **34**, 4870 (1986).
[8] M. R. Schroeder, Number Theory in Science and Communication, Springer-Verlag, Berlin, Chapter 5 (1986).
[9] N. H. McCoy, The Theory of Numbers, MacMillan, New York, p. 99 (1971).
[10] C. D. Olds, Continued Fractions, Math. Assoc. America, p. 56 (1963).
[11] P. H. Bottelberghs and G. H. J. Broers, J. Electroanal. Chem. **67**, 155 (1976).
[12] A. Lakhtakia, R. Messier, V. V. Varadan, and V. K. Varadan, Phys. Lett. A **118**, 54 (1986).
[13] J. R. MacDonald, J. Electroanal. Chem. **223**, 25, (1987).
[14] J. D. Kraus, Electromagnetics, McGraw-Hill, New York 1984, Sect. 10–16.
[15] V. K. Farkya and D. Kumar, Ind. J. Pure Appl. Phys. **24**, 592 (1986).
[16] A. Ramsamugh and F. Brouers, Phil. Mag. Lett. **55**, 301 (1987).
[17] R. Barrue, J. C. Perron, and J. Robert, Rev. Phys. Appl. (Paris) **22**, 399 (1987).
[18] A. Hessel and A. A. Oliner, Appl. Opt. **4**, 1275 (1965).
[19] A. Kapitulnik and G. Deutscher, Phys. Rev. Lett. **49**, 1444 (1982).
[20] R. B. Laibowitz, E. I. Allessandrini, and G. Deutscher, Phys. Rev. B **25**, 2965 (1982).
[21] R. F. Voss, R. B. Laibowitz, and E. I. Allessandrini, Phys. Rev. Lett. **49**, 1441 (1982).
[22] R. Messier and J. E. Yehoda, J. Appl. Phys. **58**, 3739 (1985).
[23] R. Messier, J. Vac. Sci. Technol. A **4**, 490 (1986).
[24] W. B. Jones and W. J. Thron, Continued Fractions: Analytic Theory and Applications, Addison-Wesley, Reading, Mass. 1980.